

# Global thermal entanglement in $n$ -qubit systems

R. Rossignoli, N. Canosa

*Departamento de Física, Universidad Nacional de La Plata, C.C.67, La Plata (1900), Argentina*

We examine the entanglement of thermal states of  $n$  spins interacting through different types of  $XY$  couplings in the presence of a magnetic field, by evaluating the negativities of all possible bipartite partitions of the whole system and of subsystems. We consider both the case where every qubit interacts with all others and where just nearest neighbors interact in a one-dimensional chain. Limit temperatures for non-zero negativities are also evaluated and compared with the mean field critical temperature. It is shown that limit temperatures of global negativities are strictly independent of the magnetic field in all  $XXZ$  models, in spite of the quantum transitions that these models may exhibit at zero temperature, while in anisotropic models they always increase for sufficiently large fields. Results also show that these temperatures are higher than those limiting pairwise entanglement.

PACS numbers: Pacs: 03.65.Ud, 03.67.-a, 75.10.Jm

## I. INTRODUCTION

Quantum entanglement [1] is one of the most fundamental and intriguing features of composite quantum systems, whose potential for developing radically new forms of information transmission, processing and storage was only recently recognized [2–5]. Interest on the subject has therefore grown considerably in recent years, but many aspects of entanglement, particularly in mixed states of  $n$ -component systems, are still not fully understood. Thermal entanglement [6, 7] refers normally to that of mixed states of the form  $\rho(T) \propto \exp[-H/T]$ , with  $T$  the temperature and  $H$  the system Hamiltonian, which are for instance the natural initial states in NMR based quantum computing [5].

A mixed state  $\rho$  of a two component system  $A + B$  is said to be entangled if it cannot be written as  $\sum_{\alpha} q_{\alpha} \rho_A^{\alpha} \otimes \rho_B^{\alpha}$ , with  $q_{\alpha} > 0$  and  $\rho_{A,B}^{\alpha}$  density matrices for each component [8]. If such an expansion is feasible,  $\rho$  is termed separable or classically correlated, since it is a statistical mixture of product densities and the correlations between  $A$  and  $B$  are then amenable to a classical description. A separable pure state ( $\rho^2 = \rho$ ) is always a product state  $\rho_A \otimes \rho_B$ , but this is not necessarily the case for mixed states, where it is in general difficult to prove separability. Moreover, in contrast with pure states [9], there is no unambiguous computable measure of the entanglement of mixed states, except for two-qubit systems [10]. Nonetheless, it is known that any state of a  $d$ -dimensional system is separable if it is sufficiently close to the fully mixed state  $I_d/d$  [11–13] (i.e., if  $\text{Tr}(\rho - I_d/d)^2 \leq [d(d-1)]^{-1}$  in bipartite systems [13]). This ensures the existence of a *finite limit temperature* for entanglement in any finite interacting system, above which  $\rho(T)$  becomes separable.

The situation is more complex in  $n$ -component systems [14], where there are first many possible bipartite splittings (bipartitions) of the whole system to be considered. In addition, the separability of all bipartitions does not warrant the representation of  $\rho$  as a convex combination of  $n$ -product densities  $\otimes_{i=1}^n \rho_i$  (full separability),

nor of  $m$ -product ( $2 < m < n$ ) densities ( $m$ -separability) [14]. There are as well many  $m$ -component ( $m < n$ ) subsystems whose reduced densities may similarly possess different levels of entanglement. Given the lack of simple global measures, many studies of interacting spin systems have then focused just on the entanglement of the reduced pair density, which, though physically very important, constitutes just a single aspect of the problem and leaves open the question about the entanglement of the system as a whole.

The aim of this work is to study in more detail the thermal entanglement of  $n$ -qubit systems by considering all possible bipartite splittings of the whole system, as well as of selected subsystems, and evaluating the concomitant *negativity* [11, 15–17]. This quantity is a measure of the degree of violation of the Peres criterion for separability [18, 19], and satisfies in addition some fundamental properties [17] which make it a suitable measure of bipartite entanglement in mixed states. As physical system we will consider  $n$  spins interacting through  $XYZ$  type couplings with varying anisotropies, acting either between all spins or just between nearest neighbors in a one-dimensional cyclic chain [20, 21], and embedded in a uniform magnetic field. These models are significant for solid-state based qubit representations [22–27] (the former is relevant for schemes based on quantum dots electron spins [24] and Josephson junction arrays [25–27]), and many relevant studies of the two-qubit thermal entanglement in one-dimensional chains have been made [6, 7, 28–35].

The picture that will here emerge is that of a hierarchy of negativities of global and reduced bipartitions which will possess different limit temperatures. The system will loose its quantum correlations as  $T$  increases through a cascade of “transitions” that indicate the onset of separability of the different bipartitions, with reduced pair densities becoming separable before global partitions. The behavior of all negativities depends strongly on the interaction. In  $XXZ$  models, limit temperatures of global negativities are remarkably *independent* of the magnetic field, as will be demonstrated, even though the ground

state may exhibit quantum phase transitions as the field is varied, while in anisotropic  $XYZ$  models they always increase as the field increases, even though ground state entanglement decreases. This behavior confirms that observed in two-qubit systems [32, 35]. Comparison with the mean field critical temperature will also be made, and shows that symmetry-breaking mean field solutions are not necessarily indicators of entanglement for  $T > 0$ .

## II. FORMALISM

We consider  $n$  qubits or spins coupled through an  $XYZ$  type interaction in the presence of a uniform magnetic field along the  $z$  axis. The Hamiltonian is

$$H = bS_z - \sum_{i<j} (v_x^{ij} s_x^i s_x^j + v_y^{ij} s_y^i s_y^j + v_z^{ij} s_z^i s_z^j) \quad (1a)$$

$$= H_z - \sum_{i<j} (v_+^{ij} s_+^i s_+^j + v_-^{ij} s_-^i s_-^j + h.c.), \quad (1b)$$

where  $s^i$  are the spin operators,  $S_z = \sum_{i=1}^n s_z^i$  is the total spin  $z$ -component,  $s_\pm^i = s_x^i \pm s_y^i$ ,  $v_\pm^{ij} = \frac{1}{4}(v_x^{ij} \pm v_y^{ij})$  and  $H_z = bS_z - \sum_{i<j} v_z^{ij} s_z^i s_z^j$ . We will consider two types of interaction range: I) that where every spin interacts identically with all others ( $v_\alpha^{ij} = v_\alpha \forall i < j$  and  $\alpha = x, y, z$ ) and II) that where only nearest-neighbors interact within a 1D cyclic chain ( $v_\alpha^{ij} = (\delta_{j,i+1} + \delta_{i1}\delta_{jn})v_\alpha$  for  $i < j$  and  $\alpha = x, y, z$ ). Both types become coincident for  $n = 3$ . Regardless of the interaction range,  $H$  always commutes with the  $z$ -parity or phase flip  $e^{i\pi S_z}$ , and will commute as well with  $S_z$  when  $v_x^{ij} = v_y^{ij} \forall i, j$  ( $XXZ$  models). The spectrum of  $H$  is obviously independent of the sign of  $b$  and  $v_-$  (in I and II).

For type I,  $H$  is in addition invariant against any permutation of its qubits and can be rewritten in terms of the total spin components  $S_\alpha = \sum_{i=1}^n s_\alpha^i$  as

$$H_I = bS_z - \frac{1}{2}(v_x S_x^2 + v_y S_y^2 + v_z S_z^2) + E_0, \quad (2)$$

with  $E_0 = n(v_x + v_y + v_z)/8$ . It commutes therefore with  $S^2 = \mathbf{S} \cdot \mathbf{S}$ . Its eigenvalues  $E_{SL}$  can then be obtained by diagonalizing  $H$  in each representation with total spin  $S \leq n/2$ , of dimension  $2S + 1$  and multiplicity  $Y(S) = \binom{n}{k} - \binom{n}{k-1}$ , with  $k = \frac{1}{2}n - S$  and  $Y(n/2) = 1$ , such that  $\sum_S (2S+1)Y(S) = 2^n$ . The eigenstates will be of the form  $|SL\alpha\rangle$ , with  $L = 1, \dots, 2S+1$ , and  $\alpha = 1, \dots, Y(S)$  a degeneracy index labelling different permutations. Effective pseudospin Hamiltonians of this form have been much employed in nuclear physics [36, 37], and are also suitable for describing the effective interaction of Josephson junction based charge qubits [26] as well as of quantum dots electron spins coupled through microcavity modes [24].

For type II,  $H$  is translationally invariant, and for  $v_z = 0$  it can be rewritten exactly for each  $z$ -parity as a quadratic fermionic form [21]. All  $2^n$  eigenvalues of  $H$

can then be obtained from the ensuing quasiparticle energies, determined through a fermionic Bogoliubov transformation. For even  $n$ , the spectrum of  $H$  is in this case also independent of the sign of  $v_+$ , since it can be changed just by inverting the  $x$  and  $y$  directions at odd (or even) sites.

We shall examine the entanglement of the corresponding  $n$ -qubit thermal mixed state

$$\rho = \exp[-H/T] / \text{Tr} \exp[-H/T], \quad (3)$$

by considering *all* possible bipartitions of  $k$  and  $n - k$  qubits and determining the associated *negativities* [17], defined as the absolute value of the sum of the *negative* eigenvalues of the ensuing partial transpose  $\rho^{t_p}$  of  $\rho$ :

$$N(\rho) = \frac{1}{2} \text{Tr}(|\rho^{t_p}| - \rho^{t_p}). \quad (4)$$

Here  $\rho_{ij,kl}^{t_p} = \rho_{il,kj}$ , with  $i, k$  ( $j, l$ ) labels for states of the first (second) component of the partition and  $|\rho^{t_p}| = \sqrt{(\rho^{t_p})^2}$ . According to the Peres criterion [18], if  $N(\rho) > 0$  the two components of the partition are entangled. Moreover,  $N(\rho)$  satisfies some fundamental properties of an entanglement measure [17]: It does not increase under local operations and classical communication (LOCC), being then an entanglement monotone, and is a convex function of  $\rho$  ( $N(\sum_\alpha p_\alpha \rho_\alpha) \leq \sum_\alpha p_\alpha N(\rho_\alpha)$  for  $p_\alpha \geq 0$ ,  $\sum_\alpha p_\alpha = 1$ ). It also provides an upper bound to the teleportation capacity and distillation rate [16, 17]. Not all aspects of entanglement can be captured in this way, as Peres criterion is in general sufficient only for two-qubit or qubit+qutrit systems (although entangled states satisfying  $N(\rho) = 0$  are bound entangled), and the separability of all bipartitions does not imply full separability [14]. We shall not examine these features but rather focus on  $N(\rho)$  as an indicator of useful bipartite entanglement. In the same way we will examine the entanglement of reduced densities  $\rho_m = \text{Tr}_{n-m} \rho$  for  $m < n$  selected qubits. It is apparent that for  $b \neq 0$ , entanglement in the state (3) can only be generated by the  $XY$  terms in (1a), i.e., the sum in (1b), as  $H_z$  is diagonal in the basis of separable eigenstates of  $S_z$  (standard basis).

For interactions of type I, the negativities of bipartitions with  $k$  and  $n - k$  qubits will depend just on  $n$  and  $k$ , since  $\rho$  is here completely symmetric under arbitrary permutations and any choice of the  $k$  states is equivalent. There are thus  $[n/2]$  negativities  $N_k^n (= N_{n-k}^n)$  that characterize the global bipartite entanglement (i.e.,  $N_1^3$  for  $n = 3$ ,  $N_1^4$  and  $N_2^4$  for  $n = 4$ ).

Reduced densities  $\rho_m$  for  $m < n$  qubits in I will also depend just on  $m$ , as any choice of the  $m$  states is equivalent, and will be as well completely symmetric. We have then  $[m/2]$  negativities  $N_k^m$  of reduced bipartitions with  $m$  and  $m - k$  qubits. Note that all negativities of reduced densities can be zero even if  $N_k^n > 0 \forall k$ , as occurs for the well-known GHZ type pure states  $(|0 \dots 0\rangle + |1 \dots 1\rangle)/\sqrt{2}$ , which lead to  $N_k^n = 1/2$  and  $N_k^m = 0$  for  $m < n \forall k$ . On the other hand, if  $N_k^n = 0 \forall k$ , then  $N_k^m = 0 \forall k$  and

$m < n$ . Actually, since tracing out a part of a local subsystem is a LOCC operation [17], we have the inequality

$$N_{k-j}^{n-j-l}(\rho) \leq N_k^n(\rho), \quad (5)$$

for  $j < k$ ,  $l < n - k$ , as the bipartition with  $k - j$  and  $n - k - l$  qubits of  $\rho_{n-j-l}$  can be obtained by tracing out  $j$  ( $l$ ) qubits from the first (second) component of a global partition with  $k$  and  $n - k$  qubits. This implies  $N_{k-j}^{n-j-l} = 0$  if  $N_k^n = 0$  and hence the ordering of limit temperatures  $T_{k-j}^{n-j-l} \leq T_k^n$  in the same system. For example,  $N_1^2 \leq N_1^3 \leq N_k^4$  for  $k = 1, 2$ .

For type II, the negativities will depend as well on the spacings between the  $j$  states of a subsystem. For instance, for  $n = 4$  ordered qubits  $abcd$  we have three global negativities:  $N_1^4 \equiv N_{a-bcd} = N_3^4$ , and  $N_2^4 \equiv N_{ab-cd}$ ,  $N_{2'}^4 \equiv N_{ac-bd}$ , corresponding to partitions with two adjacent and two non-adjacent qubits in each subsystem respectively. Reduced densities for  $m$  qubits will depend as well on the spacings between the  $m$  states, and will not be necessarily cyclic, so that all possible partitions will have to be examined. For instance, for  $m = 3$  adjacent qubits  $abc$  in a cyclic chain of  $n > 3$  qubits, we have the adjacent  $N_1^3 \equiv N_{a-bc} = N_{ab-c}$  and the non-adjacent  $N_{1'}^3 \equiv N_{b-ac}$  reduced negativities. Thus, for  $n = 4$  we have 3 global negativities, a single type of three-qubit reduced density  $\rho_3$  with two negativities, and 2 two-qubit densities  $\rho_2, \rho_{2'}$  for adjacent ( $ab$ ) and non-adjacent ( $ac$ ) qubits respectively, with negativities  $N_1^2, N_{1'}^2$ . By similar arguments as above, for  $n = 4$  we obtain the hierarchies  $N_{1,1'}^3 \leq N_1^4$ ,  $N_1^3 \leq N_2^4$ ,  $N_{1'}^3 \leq N_{2'}^4$ , and  $N_1^{2,2'} \leq N_{1'}^3$ ,  $N_1^2 \leq N_{1'}^3$ .

*Independence of limit temperatures from the magnetic field when  $[H, S_z] = 0$ .* A remarkable feature of the thermal states (3) with the Hamiltonian (1) is that when  $v_-^{ij} = 0 \forall i, j$  ( $XXZ$  models), the limit temperatures of global negativities are *independent* of the applied magnetic field  $b$ , even though the negativities and the ground state entanglement are not, since in such a case the eigenstates of  $H$  do not depend on  $b$  and the field dependence of  $\rho$  can be factorized. Writing the states in the standard basis succinctly as  $|m, m'\rangle$ , where  $m$  ( $m'$ ) denotes the  $z$ -component of spin in the first (second) subsystem of a bipartition (remaining labels omitted),  $\rho^{t_p}$  will have non-zero matrix elements just between states  $|m, m'\rangle$  and  $|m + k, m' + k\rangle$ , arising from those of  $\rho$  between states  $|m, m' + k\rangle$  and  $|m + k, m'\rangle$  with the same total spin  $M = m + m' + k$ . The field dependence of these elements is contained in a factor  $e^{-bM/T}/Z(b)$ , where  $Z(b) = \text{Tr} e^{-H/T}$  is the partition function. Hence, we may write

$$\rho^{t_p}(b) = r(b) \exp[-bS_z/2T] \rho^{t_p}(0) \exp[-bS_z/2T], \quad (6)$$

with  $r(b) = Z(0)/Z(b) \neq 0$  and  $[\rho^{t_p}(0), S_z] \neq 0$ . While the field dependence of the eigenvalues of  $\rho^{t_p}(b)$  cannot always be factorized, we obtain, as  $\text{Tr} S_z = 0$ ,

$$\text{Det} \rho^{t_p}(b) = [r(b)]^{2^n} \text{Det} \rho^{t_p}(0), \quad (7)$$

implying that the condition  $\text{Det}[\rho^{t_p}(b)] = 0$ , which determines in particular the limit temperature for nonzero negativity (i.e., zero lowest eigenvalue) is the same as that for  $b = 0$ . Moreover, it is apparent from the strict positivity of  $e^{-bS_z/2T}$  for  $T > 0$  that  $\rho^{t_p}(b)$  is positive (no negative eigenvalues) if and only if  $\rho^{t_p}(0)$  is positive. A similar result for limit temperatures of negativities of reduced densities does not hold.

This result has some interesting consequences. In particular, for  $[H, S_z] = 0$  the ground state will always become separable for sufficiently large fields (i.e., the state with all spins aligned  $|0\rangle \equiv |SM\rangle$ , with  $S = |M| = n/2$ ), but the limit temperature will be the same for all fields, implying the reentry of entanglement for  $T > 0$  for such values if  $N(\rho) > 0$  at low fields. It also implies that global limit temperatures will never coincide with the mean field critical temperature since the latter depends on the magnetic field (see below).

*Negativity for large fields when  $[H, S_z] \neq 0$ .* Another important feature is that for sufficiently large  $|b|$ , the thermal density (3) will possess at least one nonzero negativity at any finite temperature  $T \ll |b|$  if  $v_-^{ij} \neq 0$  at least for some pair, implying a *divergence* of the corresponding limit temperature for  $|b| \rightarrow \infty$ . For sufficiently large fields, we may treat all interaction terms perturbatively. If  $|b| \gg T$ , the thermal density will then approach that of the ground state  $|\phi_0\rangle$ , which will be the aligned state  $|0\rangle$  plus a small perturbation, as the weight of excited states become exponentially small (of order  $e^{-|b|/T}$  or less). Assuming  $b > 0$ , up to first order in  $v_-^{ij}/b$  we have  $|\phi_0\rangle = [I + \sum_{i < j} (v_-^{ij}/2b) s_+^i s_+^j] |0\rangle$ , which is an entangled state. The negativity of a partition with  $i, j$  in different subsystems and  $v_-^{ij} \neq 0$  will then be non-zero and of order  $v_-/b$  in this limit, with  $v_-$  the order of the  $v_-^{ij}$ . For instance, in the fully connected case I we obtain, for a partition with  $k$  and  $n - k$  qubits and  $T \ll |b|$ ,

$$N_k^n \approx \frac{1}{2} \sqrt{k(n-k)} |v_-/b| \quad (8)$$

up to first order in  $v_-/b$ . Note that  $k(n - k)$  is just the number of links  $v_-^{ij}$  between the two subsystems, being  $N_k^n$  maximum for  $k = [n/2]$ . In type II, for partitions with  $k$  and  $n - k$  adjacent qubits, we obtain instead

$$N_k^n \approx \frac{1}{2} r_k |v_-/b|, \quad (9)$$

where  $r_1 = \sqrt{2}$  and  $r_k = 2$  for  $2 \leq k \leq [n/2]$ . For partitions consisting of non-contiguous qubits the value of  $r_k$  will be larger (and in fact proportional to  $n/2$  for a bipartition with  $k = [n/2]$  non-adjacent qubits in each set).

*Mean field approximation.* The thermal state (3) provides the absolute minimum of the free energy  $F(\rho) = \langle H \rangle - TS(\rho)$ , where  $\langle H \rangle = \text{Tr} \rho H$  and  $S(\rho) = -\text{Tr} \rho \ln \rho$  is the von Neumann entropy. The finite temperature mean field approximation is based on the minimization of  $F(\rho)$  within the subset of uncorrelated density opera-

tors

### III. RESULTS

$$\rho_{\text{mf}}(T) = \exp[-h/T] / \text{Tr} \exp[-h/T], \quad h = \sum_{i=1}^n \lambda_i \cdot \mathbf{s}^i. \quad (10)$$

This leads to the self-consistent equations  $\lambda_i = \partial \langle H \rangle_{\text{mf}} / \partial \langle \mathbf{s}^i \rangle_{\text{mf}}$ , with  $\langle O \rangle_{\text{mf}} = \text{Tr} \rho_{\text{mf}} O$ , which determine a  $T$  dependent (and possibly symmetry-breaking) effective non-interacting hamiltonian  $h$ . For  $v_z = 0$  and  $v_x \geq 0$ , with  $|v_y| \leq v_x$ , it suffices to consider  $h = bS_z - \lambda S_x$ . The limit temperature of the ensuing  $z$ -parity symmetry breaking solution ( $\lambda \neq 0$ ) is

$$T_c = |b| / \ln \left[ \frac{\eta + 1}{\eta - 1} \right], \quad \eta \equiv v/|b| > 1, \quad (11)$$

where  $v = v_x(n-1)/2$  in I and  $v = v_x$  in II. For fixed  $v$ , the mean field solution and intensive energy

$$\langle H \rangle_{\text{mf}} / n = b \langle s_z \rangle_{\text{mf}} - v \langle s_x \rangle_{\text{mf}}^2 \quad (12)$$

are hence the same in I and II, and are independent of the number of qubits  $n$  and of  $v_y$ .

For  $\eta \gg 1$  (low fields  $|b| \ll v$ ),  $T_c/v = \frac{1}{2} + O(\eta^{-2})$ , while for  $\eta \leq 1$  ( $|b| \geq v$ ),  $T_c = 0$  (i.e.,  $\lambda = 0 \forall T$ ) and no interaction is “seen” at the mean field level. This implies that at least for  $|b| > v$ , there will be no agreement between  $T_c$  and the limit temperatures for global negativities even for *large*  $n$ , as the latter either stay constant ( $XXZ$  models) or tend to increase (full anisotropic models) for increasing fields. Note also from Eq. (8) that for large fields ( $\eta \ll 1$ ), the negativity of symmetric global partitions ( $k = n/2$ ) in anisotropic models of type I remains non-zero for  $n \rightarrow \infty$  even if  $v_- \propto v/n$ , and the same occurs in type II models (for  $v_- \propto v$ ), explaining thus the lack of agreement with  $T_c$ . Nevertheless, for  $\eta > 1$  limit temperatures for global negativities will typically be of the same order as  $T_c$ , as will be seen in the next section.

Let us note as well that in the fully connected case I, the strength of the common pair coupling  $v^{ij} = 2v/(n-1)$  between spins  $s^i, s^j$  required for symmetry breaking at finite temperature or field scales as  $n^{-1}$ , becoming then smaller than in an array of type II as  $n$  increases. Thus, at the mean field level weak pair couplings in I have the same effect as much stronger values in II. Typical values of  $v^{ij}$  can be of order  $4\tilde{g}_{ij} \approx 0.08$  meV for quantum dots electron spins coupled through a microcavity mode [24], while in Josephson charge qubits arrays [25],  $v_{ij} = 4E_J^i E_J^j / E_L \approx 40mK$  (in temperature units) for  $E_L = 10E_J$ , where  $E_J^i \propto E_J \approx 100mK$  are the effective Josephson energies of the qubits controlled by the external fluxes and  $E_L$  an energy scale depending on the SQUID inductance  $L$ . For  $|b| \approx E_J$  we have then  $\eta \approx 0.2(n-1)$  and  $T_c \approx \frac{1}{2}v \approx 10mK(n-1)$  for  $\eta \gtrsim 2$ .

We discuss now numerical results for the  $XY$  case ( $v_z = 0$ ) with  $v_x \geq 0$  and different anisotropies  $v_-/v_+ = (v_x - v_y)/(v_x + v_y)$ , for interactions of types I and II. We first consider the thermal behavior in the fully anisotropic case  $v_y = -v_x$  ( $v_+ = 0$ ), because it is the simplest to describe and represents that of a system with a non-degenerate entangled ground state well separated from the remaining states, which depends smoothly on the magnetic field. Typical results for  $n = 3, 4, 6$  and  $\eta = v/|b| = 2$  are shown in fig. 1. For  $n = 3$ , there is a single global negativity  $N_1^3 = N_2^3$ , which decreases monotonously as  $T$  increases, vanishing at  $T_1^3 \approx 0.77v$ , while the negativity  $N_1^2$  of the reduced two-qubit density is smaller and vanishes at  $T_1^2 \approx 0.54v$ . Hence, there is an appreciable interval  $[T_1^2, T_1^3]$  where only global entanglement persists. Both  $T_1^3$  and  $T_1^2$  are *higher* than the mean field critical temperature  $T_c \approx 0.46v$ , although of the same order, and negativities are actually rather small above  $T_c$ . The mean value of the interaction  $\langle V \rangle \equiv \text{Tr} \rho V$ , where  $V$  denotes the sum in Eq. (1), remains however quite significant for  $T > T_1^3$ , vanishing only for  $T \rightarrow \infty$ , which indicates that  $\rho$  remains considerably correlated for  $T > T_1^3$  albeit in an essentially classical manner.

The behavior for  $n = 4$  and 6 qubits is similar. For type I interaction (left panels) and  $n = 4$ , there are just two global negativities,  $N_1^4, N_2^4$ , the latter being the strongest and most persistent ( $(T_1^4, T_2^4) \approx (0.62, 0.72)v$ ). This difference can be attributed to the higher number of links  $v^{ij}$  between both subsystems existing in the latter (4 for  $N_2^4$  and 3 for  $N_1^4$ ). The negativities  $N_1^3$  and  $N_1^2$  of the reduced three- and two-qubit densities are smaller, in agreement with (5), and vanish at  $(T_1^3, T_1^2) \approx (0.52, 0.41)v$  (which are lower than those of the upper panel). There is again an interval  $[T_1^3, T_2^4]$  where only *global* negativities  $N_1^4, N_2^4$  are non zero, and a smaller interval  $[T_1^4, T_2^4]$  where just *one* global negativity survives. For  $n = 6$  we obtain similarly a cascade of limit temperatures  $(T_1^6, T_2^6, T_3^6) \approx (0.54, 0.6, 0.64)v$  for the global negativities  $N_1^6, N_2^6, N_3^6$ , the latter being the greatest and most persistent in agreement with the number of links (5, 8 and 9 respectively). There is as well a series of lower limit temperatures  $(T_1^2, T_1^3, T_1^4, T_2^4, T_1^5, T_2^5) \approx (0.31, 0.36, 0.41, 0.45, 0.47, 0.53)v$  for the negativities of reduced densities  $\rho_m$ . Just the most persistent one for each  $m$  ( $N_{[m/2]}^m$ ) is shown. Note that  $N_2^5 \approx N_1^6$  for  $T \gtrsim 0.2v$ , as  $N_2^5$  is not necessarily smaller than  $N_1^6$ .

The behavior for type II interaction is similar, although limit temperatures are higher (in comparison with the corresponding value of  $v$  or  $T_c$ ). For  $n = 4$  qubits  $abcd$ , there are three different global negativities, the most persistent being that of the *non-adjacent* 2+2 partition  $N_2^4 = N_{ac-bd}$ , followed by  $N_1^4 = N_{a-bcd}$  and finally that of the adjacent partition  $N_2^4 = N_{ab-cd}$ . The latter, though coincident with the first one at  $T = 0$ , decays faster:  $(T_2^4, T_1^4, T_2^4) \approx (0.71, 0.78, 0.96)v$ . This is again in agreement with the number of links between subsys-

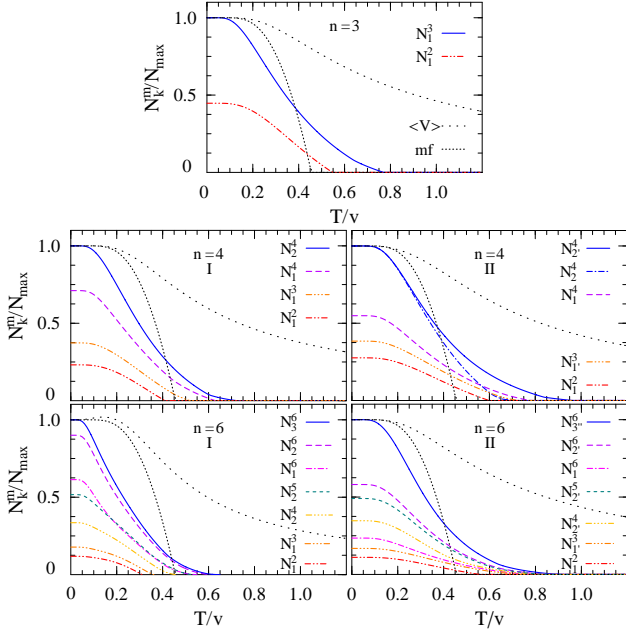


FIG. 1: Thermal behavior of the negativities determined by the state (3) for  $n = 3, 4$  and  $6$  qubits, for an  $XY$  interaction with  $v_y = -v_x$  ( $v_+ = 0$ ) and  $v/b = 2$ . Results for both the full (I) and cyclic nearest neighbor (II) interaction ranges, coincident for  $n = 3$ , are depicted.  $N_k^n$  is the negativity of a global bipartition with  $k$  and  $n - k$  qubits, while for  $m < n$ ,  $N_k^m$  is that of a reduced density for  $m$  qubits, adjacent in II.  $N_{\max}$  is the largest negativity at  $T = 0$  and primes in panels II denote different bipartitions (see text). Also shown for reference are the exact thermal average of the interaction ( $\langle V \rangle$ ) and its mean field average (mf), both scaled for clarity to their  $T = 0$  values.

tems (4 for  $N_2^4$ , 2 for  $N_2^4$  and  $N_1^4$ ). The reduced pair density of adjacent qubits  $ab$  remains now entangled until  $T_1^2 \approx 0.59v$ , while that of two non-adjacent qubits  $ac$  is here *separable*  $\forall T$  ( $N_1^{2'} = 0$ ). The reduced three-qubit density has here two negativities:  $N_1^3 = N_{a-bc}$  and  $N_3^3 = N_{ac-b}$ , the latter being the most persistent:  $(T_1^3, T_3^3) \approx (0.62, 0.72)v$ . Just  $N_1^3$  is shown. We have then the ordering  $T_1^2 < T_1^3 < T_2^4 < T_1^{3'} < T_1^4 < T_2^4$ . Note that  $N_2^4$  is not necessarily greater than  $N_1^{3'}$ .

For  $n = 6$  qubits  $abcdef$  there are 7 global negativities for type II:  $N_1^6 = N_{ab-cdef}$ ,  $N_2^6 = N_{ab-cdef}$ ,  $N_2^{6'} = N_{ac-bdef}$ ,  $N_2^{6''} = N_{ad-bcef}$ , and  $N_3^6 = N_{abc-def}$ ,  $N_3^{6'} = N_{abd-cef}$ ,  $N_3^{6''} = N_{ace-bdf}$ . The most persistent is that of the non-contiguous 3+3 partition  $N_3^{6''}$  (6 links), followed by  $N_2^6$  (4 links), with  $(T_3^{6''}, T_2^6) \approx (0.95, 0.87)v$ , whereas those of adjacent qubits,  $N_1^6$ ,  $N_2^6$  and  $N_3^6$  (2 links), are the first to vanish:  $(T_1^6, T_2^6, T_3^6) \approx (0.77, 0.71, 0.7)v$ . Only the most persistent of each  $N_k^6$  set is depicted. Also shown are the most persistent negativities of reduced densities of adjacent qubits, which are again those of most symmetric partitions with non-adjacent qubits:  $N_1^{3'}$  for  $\rho_3$  and  $N_2^{4'} = N_{ac-bd}$ ,  $N_2^{5'} = N_{bd-ace}$  for  $\rho_4, \rho_5$  (which have 5 and 9 different negativities). We obtain the ordering

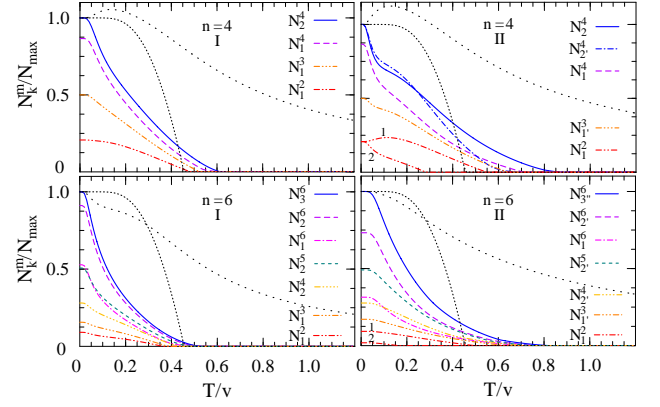


FIG. 2: Same quantities as fig. 1 for  $v_y = v_x$  ( $v_- = 0$ ). Details are the same as before. Right panels results for the reduced density of both adjacent (I) and first non-adjacent (II) pairs. The latter vanished in fig. 1.

$$T_1^2 < T_1^{3'} < T_1^6 < T_2^4 < T_2^{5'} < T_2^6 < T_3^{6''}.$$

Results for the  $XX$  case  $v_x = v_y$  ( $v_- = 0$ ) are shown in fig. 2. Here the eigenstates of  $H$  have definite values  $M$  of  $S_z$  and first order ground state transitions  $|M| \rightarrow |M| + 1$  arise as  $|b|$  increases (see fig. 3 and the ensuing description). For  $\eta = 2$  the ground state has  $|M| = 1$  for  $n = 4$  and  $n = 6$ , and is entangled and non-degenerate. The ensuing thermal behavior is, accordingly, roughly similar to the previous case (results for  $n = 3$ , not shown, are very similar to those of fig. 1). However, for  $n = 4$  and  $6$  we observe a more rapid initial decrease of *global* negativities with increasing temperature, particularly noticeable for  $n = 4$  in case II. This is due to the presence of a low lying entangled first excited state, which becomes then mixed with the ground state already at low  $T < T_c$ , thus reducing the negativity. Note that in contrast, the thermal average of the interaction  $\langle V \rangle$  *increases* initially with temperature for  $n = 4$ , since in this case this state has  $M = 0$  and is more correlated than the ground state. For  $n = 6$  this state has instead  $|M| = 2$  and weaker correlations, so that  $\langle V \rangle$  also exhibits here an initial decrease. Another novel aspect is the appearance of a small non-zero negativity for the first non-adjacent pair density (qubits  $ac$ ) in case II (right panels), which vanishes at a low  $T$ . All other limits temperatures are slightly lower than those of fig. 1, although the ordering of those depicted remains unchanged.

Fig. 3 offers a global view of the behavior with temperature and magnetic field of the most persistent negativity for  $n = 6$  ( $N_3^6$ ), for increasing anisotropies in a type I interaction. For  $v_x = v_y$  (a), global negativities exhibit a *stepwise* increase at  $T = 0$  as  $\eta$  increases, reflecting the ground state transitions  $|M| \rightarrow |M| - 1$ . The exact energies are in this case given by (Eq. (2))

$$E_{SM} = bM - v[S(S+1) - M^2]/(n-1) + E_0,$$

so that for  $v > 0$  the ground state corresponds to  $S = n/2$  and  $|M|$  determined by the ratio  $\eta = v/|b|$ . For  $b > 0$ , a

total of  $[n/2]$  transitions  $M \rightarrow M + 1$  occur therefore at

$$\eta = (n - 1)/(2|M| - 1),$$

where  $E_{SM} = E_{S,M+1}$ , with  $M = -n/2$  for  $\eta < 1$  (aligned state). The first transition at  $\eta = 1$  marks then the appearance of entanglement at  $T = 0$  (with  $N_k^n = \sqrt{k(n-k)}/n$  for  $M = -n/2 + 1$ ) and coincides with the onset of the symmetry-breaking mean field solution. For  $n = 6$ , the transitions occur at  $\eta = 1, \frac{5}{3}, 5$ .

For  $T \rightarrow 0$ , entanglement starts then only for  $\eta > 1$  and exhibits drops at the critical ratios due to the degeneracy of the ground state. At fixed low  $T > 0$ , global negativities display accordingly smooth minima around these values. Limit temperatures of global negativities are however independent of  $b$  in this case, so that for  $\eta < 1$  the system becomes entangled only for  $T > 0$ , as in the two-qubit case [7, 35], although negativities are very small.

For small but non-zero anisotropies  $v_-/v_+$ , ground state transitions persist (leading to discontinuities in  $\langle S_z \rangle$  and the negativities), but the ground state is no longer constant between transitions. The associated negativities begin to vary smoothly between them and start already for  $v > 0$ , increasing linearly with  $\eta$  for  $\eta \ll 1$ , following Eq. (8). At the same time, the limit temperature is no longer constant and the negativity becomes non-zero for  $\eta \rightarrow 0$  at any  $T \ll b$ . The concomitant behavior can be appreciated in panel (b) for  $v_-/v_+ = \frac{1}{2}$  ( $v_y = v_x/3$ ) where the ground state transitions occur at  $\eta \approx 1.73, 2.88$  and  $8.66$ . For small  $\eta$  we observe the tail corresponding to the entanglement of the perturbed aligned state, while above the first transition the negativity undergoes an abrupt initial decrease as  $T$  increases from 0 due to the almost degeneracy of the ground state. Note also that at low  $T > 0$ ,  $N_3^6$  displays a deep minimum in the vicinity of the first transition as  $\eta$  increases.

For  $v_-/v_+ = 1$  ( $v_y = 0$ ), the ground state transitions disappear, although the energies of the ground and first excited states become almost degenerate for large  $\eta$  (where they approach the states  $(|S, M_x\rangle \pm |S, -M_x\rangle)/\sqrt{2}$  with  $M_x = S = n/2$  and  $|S, M_x\rangle$  the eigenstates of  $S^2$  and  $S_x$ ), with an energy splitting  $\Delta E \propto v\eta^{-n}$  in this limit. This leads again to a rapid initial drop of the negativity as  $T$  increases from 0. The final effect for low  $T > 0$  and  $\eta \gtrsim 1$  is a *decrease* of the negativity for increasing  $\eta$ . Finally, the behavior in the fully anisotropic case  $v_-/v_+ = \infty$  ( $v_y = -v_x$ ) is completely smooth as either  $T$  or  $\eta$  increases. All global negativities increase as  $\eta$  increases at  $T = 0$  and decrease smoothly as  $T$  increases.

The corresponding results for the type II interaction (fig. 4) exhibit the same behavior. The most persistent negativity in all cases depicted is that of the non-adjacent 3+3 partition  $N_{3''}^6 = N_{ace-bdf}$ , which for  $\eta \rightarrow 0$  and  $T \ll b$  increases for non-zero anisotropy as in Eq. (9) with  $r_k = 4$  (for the other partitions  $N_{2'}^6, N_{2''}^6, N_{3'}^6$  we have  $r_k = 1 + \sqrt{3}, 2\sqrt{2}, 1 + \sqrt{5}$  respectively). In the  $XX$  case (panel a), the ground state exhibits again three transitions  $M \rightarrow M+1$  at  $\eta = 1, 1/(\sqrt{3}-1) \approx 1.37$  and  $1/(2-\sqrt{3}) \approx 3.73$ ,

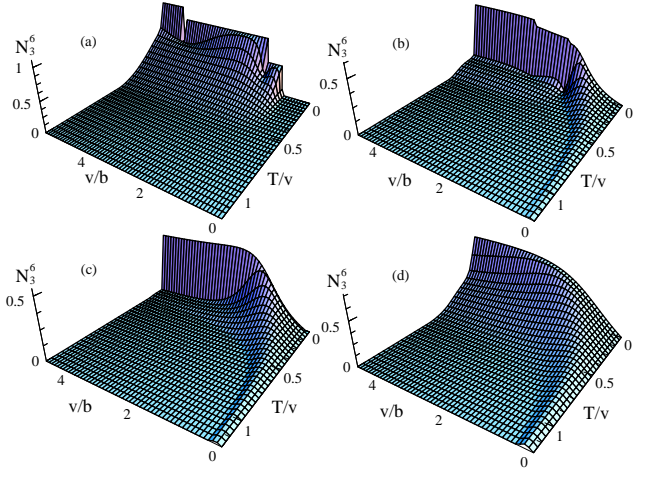


FIG. 3: The most persistent global negativity as a function of temperature and inverse magnetic field for  $n = 6$  and the full range interaction I, with  $v_-/v_+ = 0$  (a),  $1/2$  (b),  $1$  (c) and  $\infty$  (d).

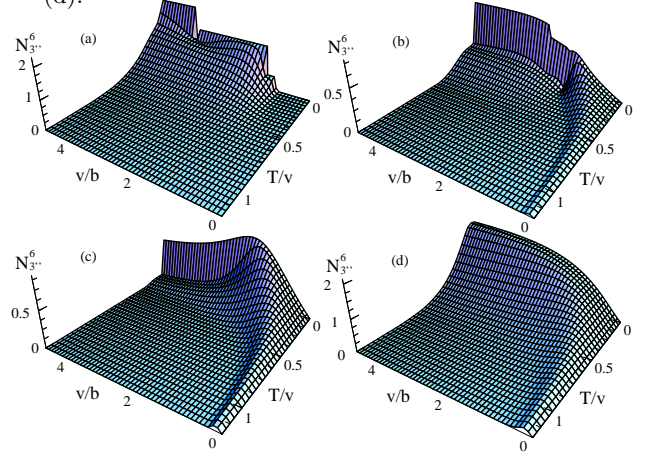


FIG. 4: Same quantities and details as in fig. 3 for the nearest neighbor interaction II.

corresponding to energies  $E_{-3} = -3b$ ,  $E_{-2} = -2b - v$ ,  $E_{-1} = -b - \sqrt{3}v$  and  $E_0 = -2v$ , where  $E_M$  denotes the lowest energy for a given  $M$ . The first transition occurs again at the same value  $\eta = 1 \forall n$ , and the ground state for  $\eta < 1$  is again the aligned state, so that the  $T = 0$  negativity starts only for  $\eta > 1$  and increases stepwise. For  $v_-/v_+ = 1/2$  (b) the transitions occur at  $\eta \approx 1.73, 2.31$  and  $6.28$ . The negativity exhibits in this case a non-monotonous behavior at  $T = 0$ , showing a maximum and a minimum just before the first transition, the latter becoming very pronounced as  $T$  increases. The same previous effects are seen for  $v_-/v_+ = 1$  (c), where the energy gap  $\Delta E$  between the ground and first excited states decreases again as  $v\eta^{-n}$  for  $\eta \gg 1$ , while for  $v_y = -v_x$  (d) the behavior is again completely smooth.

Beneath the surfaces of figs. 3-4 lie those of the remaining global and reduced negativities. We plot in fig. 5 the corresponding main limit temperatures for type I interaction. As previously shown, in the  $XX$  case (panels a)  $T_k^n/v$  is constant for all global negativities. This is also approximately true for limit temperatures of all reduced



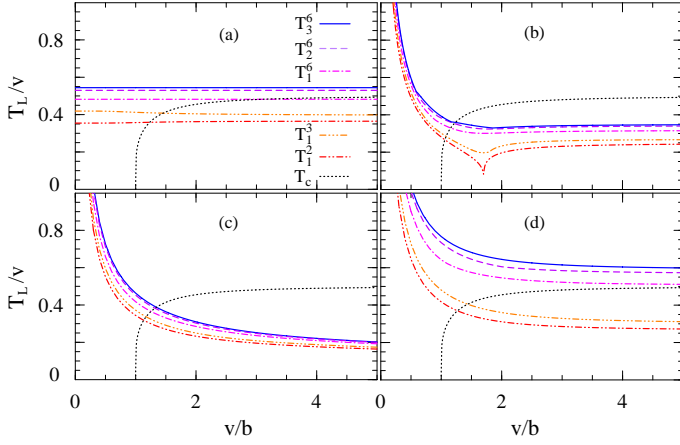


FIG. 5: Limit temperatures  $T_L \equiv T_k^m$  for non-zero negativities  $N_k^m$ , for the full range interaction I with  $v_-/v_+ = 0$  (a),  $1/2$  (b),  $1$  (c) and  $\infty$  (d). The dotted line depicts the mean field critical temperature  $T_c$ .

negativities in I. However, for non-zero anisotropies (panels b,c,d), *all* limit temperatures in I diverge for  $\eta \rightarrow 0$ , in agreement with our previous discussion. This is in marked contrast with the behavior of the mean field critical temperature, which vanishes for  $\eta < 1$ . Limit temperatures are not, however, proportional to  $|b|$  in this limit and ratios  $T_k^n/|b|$  actually vanish for  $\eta \rightarrow 0$ .

Whereas in panels (a) and (d) limit temperatures of global negativities become close to  $T_c$  for large  $\eta$ , in (b) and particularly c) they become substantially *lower* than  $T_c$ , due to the quasi-degeneracy of the two lowest energy levels in this region. This indicates that symmetry-breaking is not necessarily an indication of entanglement at finite temperature. Besides, limit temperatures *are not necessarily smooth functions of  $\eta$* , as occurs for instance in case (b), where  $T_3^6$  exhibits two slope discontinuities at  $\eta \approx 1.17$  and  $1.83$ , being minimum at the last value. These transitions reflect the changes in the lowest eigenvalue of  $\rho^{t\nu}$ , arising from level crossings, and become more noticeable in the limit temperatures of reduced negativities, as seen for  $T_1^3$  and particularly  $T_1^2$ , which exhibits a deep minimum at  $\eta \approx 1.7$ . The thermal behavior of the associated negativity in the vicinity of these crossovers can be more complex than in figs. 1-2, and may exhibit a deep minimum followed by a maximum before vanishing, which may even evolve into a complete vanishing plus a reentry.

Results for type II interaction (fig. 6) are quite similar. Limit temperatures of global negativities and of reduced densities of adjacent qubits are higher than in I for the same value of  $v$ , although they exhibit the same behavior and still fall well below  $T_c$  in (c). With the exception of case (d), reduced pair densities of *non-adjacent* qubits (i.e., (a,c) (2) and (a,d) (3)) have as well non-zero negativities at least for some field intervals, although they possess low limit temperatures that depend strongly on the magnetic field even in (a). For  $n = 6$ , qubits (a,c) in (a) are entangled at  $T = 0$  just between the first and third

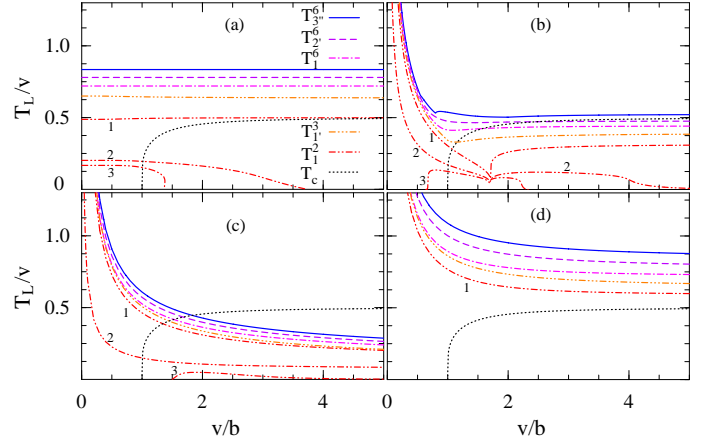


FIG. 6: Same quantities and details as in fig. 5 for the nearest neighbor interaction II. Labels 1,2,3 indicate results for the adjacent and the two first non-adjacent pair densities respectively.

transition ( $1 < \eta < 3.73$ ) while qubits (a,d) just between the first and second transition ( $1 < \eta < 1.37$ ), although for  $T > 0$  both become weakly entangled also for  $\eta < 1$  (reentry effect). Case b) is more complex since it exhibits crossovers as in type I, reflected in the appearance of minima and slope discontinuities in the limit temperatures. The highest one  $T_{3''}^6$  has minima with slope discontinuities at  $\eta \approx 0.8$  and  $1.99$ , the latter being the absolute minimum. That of the reduced density of adjacent qubits displays actually a discontinuity at the minimum which is the signature of a *reentry effect* (for  $1.71 \lesssim \eta \lesssim 1.72$ ,  $N_1^2$  exhibits a small reentry as  $T$  increases after its first zero, originating a discontinuity in the final limit temperature at  $\eta \approx 1.71$ ). Those of non-adjacent qubits *ac* (2) and *ad* (3) exhibit the same behavior in the vicinity of  $\eta = 1.7$ . That of qubits *ac* becomes infinite for  $\eta \rightarrow 0$ , like  $T_1^2$ , but vanishes after the third  $T = 0$  transition ( $\eta \gtrsim 6.28$ ), while that of *ad* is non-zero just for  $0.68 \lesssim \eta \lesssim 2.31$  (below the second  $T = 0$  transition). In c) qubits *ac* become entangled  $\forall \eta > 0$ , and their limit temperature, though lower, exhibits the same behavior as that of adjacent qubits, while qubits *ad* become entangled just for  $\eta \gtrsim 1.5$  up to a very low temperature. Finally, in d) non-adjacent pairs become separable, while the other limit temperatures become all higher than  $T_c$ .

#### IV. CONCLUSIONS

In this work we have investigated the thermal entanglement of  $n$ -spin systems by evaluating the set of negativities associated with all possible bipartite splittings of the system and subsystems. Entanglement is then seen to decay for increasing  $T$  through a cascade of limit temperatures that determine the onset of separability of the different bipartitions. For the cases here considered, the most persistent global negativity is that of the most symmetric bipartition ( $N_{[n/2]}^n$ ) in the fully connected case I,

and the same occurs in the nearest neighbor case II provided *non-contiguous* qubits are chosen in each partition. Negativities of reduced densities and of weakly interacting splittings vanish obviously earlier, so that there is always some final interval where only *global* entanglement survives. The behavior with temperature and magnetic field of the most persistent negativity is rather similar in I and II for the cases considered after adequate scaling of coupling strengths ( $v_{ij} \propto v/n$  in I and  $\propto v$  in II) but depends strongly on the anisotropy.

In all  $XXZ$  models, we have shown that limit temperatures of global negativities are *strictly independent* of the (uniform) applied magnetic field  $b$ , for *any* value of the total qubit number  $n$ , even though the negativity may exhibit a stepwise variation with the field at  $T = 0$ . This implies in particular that one cannot expect an agreement for all fields between these limit temperatures and the mean field critical temperature  $T_c$ , even for *large*  $n$ , as the latter always *vanishes* for sufficiently large fields. The lack of agreement persists in anisotropic models, where limit temperatures for global entanglement were shown to become large for large fields, even though the nega-

tivity tends to zero in this limit. In this case we have shown explicitly that for large fields ( $\eta < 1$ ) and sufficiently low  $T$ , negativities of most symmetric partitions remain finite even for large  $n$  (Eqs. (8)-(9)). Nevertheless, for  $\eta > 1$  the negativity is normally seen to become relatively small above  $T_c$  (figs. 1-2), so that in this sense an approximate agreement with the mean field picture is recovered. Negativities may also vanish for  $T < T_c$  when ground state degeneracies (exact or approximate) are present, as seen in cases b and c in figs. 5-6. Finally, it is to be remarked that limit temperatures may exhibit slope or full discontinuities for increasing fields for finite anisotropies, reflecting crossovers between different entanglement regimes, which may become more pronounced for those of reduced negativities. The present study provides therefore a more complete understanding of the way finite spin systems loose their quantum correlations due to standard (i.e., Boltzmann like) thermal randomness. Other aspects of the problem are presently under investigation.

*Acknowledgments.* RR and NC acknowledge support, respectively, from CIC and CONICET of Argentina.

- 
- [1] E. Schrödinger, *Naturwissenschaften* **23**, 807 (1935); *Proc. Cam. Philos. Soc.* **31**, 555 (1935).
  - [2] C.H. Bennett et al., *Phys. Rev. Lett.* **70**, 1895 (1993); *Phys. Rev. Lett.* **76**, 722 (1996).
  - [3] D.P. DiVincenzo, *Science* **270**, 255 (1995).
  - [4] C.H. Bennett and D.P. DiVincenzo, *Nature (London)* **404**, 247 (2000).
  - [5] M.A. Nielsen and I. Chuang, *Quantum Computation and Quantum Information*, Cambridge Univ. Press (2000).
  - [6] M.A. Nielsen, Ph.D. thesis, Univ. of New Mexico, 1998 (unpublished); quant-ph/0011036.
  - [7] M.C. Arnesen, S. Bose and V. Vedral, *Phys. Rev. Lett.* **87**, 017901 (2001).
  - [8] R.F. Werner, *Phys. Rev. A* **40**, 4277 (1989).
  - [9] C.H. Bennett, H.J. Bernstein, S. Popescu, and B. Schumacher, *Phys. Rev. A* **53**, 2046 (1996).
  - [10] S. Hill and W.K. Wootters, *Phys. Rev. Lett.* **78**, 5022 (1997); W.K. Wootters, *Phys. Rev. Lett.* **80**, 2245 (1998).
  - [11] K. Życzkowski, P. Horodecki, A. Sanpera, and M. Lewenstein, *Phys. Rev. A* **58**, 883 (1998).
  - [12] S.L. Braunstein et al., *Phys. Rev. Lett.* **83**, 1054 (1999).
  - [13] L. Gurvits and H. Barnum, *Phys. Rev. A* **66**, 062311 (2002); *Phys. Rev. A* **68**, 042312 (2003).
  - [14] W. Dür, J.I. Cirac and R. Tarrach, *Phys. Rev. Lett.* **83**, 3562 (1999); W. Dür and J.I. Cirac, *Phys. Rev. A* **61**, 042314 (2000).
  - [15] K. Życzkowski, *Phys. Rev. A* **60**, 3496 (1999).
  - [16] M. Horodecki, P. Horodecki, and R. Horodecki, *Phys. Rev. Lett.* **84**, 4260 (2000).
  - [17] G. Vidal and R.F. Werner, *Phys. Rev. A* **65**, 032314 (2002).
  - [18] A. Peres, *Phys. Rev. Lett.* **77**, 1413 (1996).
  - [19] M. Horodecki, P. Horodecki, and R. Horodecki, *Phys. Lett. A* **223**, 1 (1996).
  - [20] A. Sachdev, *Quantum Phase Transitions*, Cambridge Univ. Press (1999).
  - [21] E. Lieb, T. Schultz and D. Mattis, *Ann. Phys. (NY)* **16**, 407 (1961).
  - [22] D. Loss and D.P. DiVincenzo, *Phys. Rev. A* **57**, 120 (1998).
  - [23] G. Burkard, D. Loss, and D.P. DiVincenzo, *Phys. Rev. B* **59**, 2070 (1999).
  - [24] A. Imamoglu, D.D. Awschalom, G. Burkard, D.P. DiVincenzo, D. Loss, M. Sherwin, and A. Small, *Phys. Rev. Lett.* **83**, 4204 (1999).
  - [25] Y. Makhlin, G. Schön and A. Shnirman, *Nature* **398** 305 (1999); A. Shnirman, G. Schön and Z. Hermon, *Phys. Rev. Lett.* **79**, 2371 (1997).
  - [26] Y. Makhlin, G. Schön and A. Shnirman, *Rev. Mod. Phys.* **73**, 357(2001); W.A. Al-Saidi and D. Stroud, *Phys. Rev. B* **65** (224512) (2002).
  - [27] J.J. Vartiainen et al, *Phys. Rev. A* **70** 012319 (2004).
  - [28] X. Wang, *Phys. Rev. A* **64**, 012313 (2001).
  - [29] D. Gunlycke, V.M. Kendon, V. Vedral, and S. Bose, *Phys. Rev. A* **64**, 042302 (2001).
  - [30] T.J. Osborne and M.A. Nielsen, *Phys. Rev. A* **66**, 032110 (2002).
  - [31] X. Wang, *Phys. Rev. A* **66**, 044305 (2002); *Phys. Rev. A* **66**, 034302 (2002); X. Wang and P. Zanardi, *Phys. Lett. A* **301**, 1 (2002).
  - [32] G.L. Kamta and A.F. Starace, *Phys. Rev. Lett.* **88**, 107901 (2002).
  - [33] U. Glaser, H. Büttner, and H. Fehske, *Phys. Rev. A* **68**, 032318 (2004).
  - [34] Y. Sun, Y. Chen, and H. Chen, *Phys. Rev. A* **68**, 044301 (2003).
  - [35] N. Canosa, R. Rossignoli, *Phys. Rev. A* **69**, 052306 (2004).
  - [36] H.J. Lipkin, N. Meshkov, A.J. Glick, *Nucl. Phys.* **62**, 188 (1965).



- [37] P. Ring, P. Schuck, *The Nuclear Many-Body Problem*, Springer, NY (1980).